Detection of Structural Changes upon One Electron Oxidation and Reduction of Stilbene Derivatives by Time-Resolved Resonance Raman Spectroscopy during Pulse Radiolysis and Theoreti...

ARTICLE *in* THE JOURNAL OF PHYSICAL CHEMISTRY A · JUNE 2015

Impact Factor: 2.69 · DOI: 10.1021/acs.jpca.5b04127 · Source: PubMed

THE JOURNAL OF PHYSICAL CHEMISTRY A

Article

pubs.acs.org/JPCA

Detection of Structural Changes upon One-Electron Oxidation and Reduction of Stilbene Derivatives by Time-Resolved Resonance Raman Spectroscopy during Pulse Radiolysis and Theoretical Calculations

Mamoru Fujitsuka,*[,†] Dae Won Cho,[†,‡] Jungkweon Choi,[†,§] Sachiko Tojo,[†] and Tetsuro Majima*[,†]

[†]The Institute of Scientific and Industrial Research, Osaka University, Mihogaoka 8-1, Ibaraki, Osaka 567-0047, Japan

[‡]Department of Advanced Materials Chemistry, Korea University (Sejong Campus), Sejong 339-700, Korea

[§]Center for Nanomaterials and Chemical Reactions, Institute for Basic Science, Daejeon 305-701, Korea

Supporting Information

ABSTRACT: Stilbene (St) derivatives have been investigated for many years because of their interesting photochemical reactions such as cis−trans isomerization in the excited states and charged states and their relation to poly(*p*-phenylenevinylene)s. To clarify their charged state properties, structural information is indispensable. In the present study, radical cations and radical anions of St derivatives were investigated by radiation chemical methods. Absorption spectra of radical ion states were obtained by transient absorption measurements during pulse radiolysis; theoretical calculations that included the solvent effect afforded reasonable assignments. The variation in the peak position was explained by using HOMO and LUMO energy levels. Structural changes upon one-electron oxidation and reduction were detected by time-resolved resonance Raman measurements during pulse radiolysis. Significant downshifts were observed with the CC stretching mode of the ethylenic groups, indicative of the decrease in the bonding order. It was confirmed that the downshifts observed with reduction were larger than those with oxidation. On the other hand, the downshift caused by oxidation depends significantly on the electron-donating or electron-withdrawing nature of the substituents.

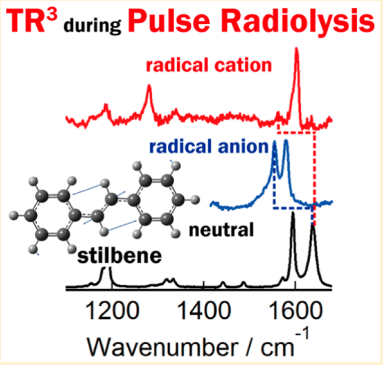

INTRODUCTION

Stilbene (St) derivatives have been investigated for many years because of their simple chemical structures and interesting photochemical reactions such as cis−trans isomerization in the excited states and charged states.[1−7] St derivatives are also regarded as the smallest unit of poly(*p*-phenylenevinylene)s, which have suitable characteristics for studying electro- and photofunctional conjugated materials.[8] It is important to understand the charged states because these states are responsible for their properties. Electronic transitions, that is, absorption spectra in the UV−vis regions of some St derivatives, have been studied by using various measurements techniques.[9] Our research group has investigated the transient absorption spectra of radical cations of stilbene derivatives to clarify their isomerization process as well as the dimerization and oxidation processes with molecular oxygen in the solvent.[10−12] The previous studies have shown the importance of charge distribution but have not provided further structural information. Note that charge distribution is essential not only for chemical reactivity in the charged state but also for charge transport in polymeric materials. To clarify these properties, investigation by means of absorption measurements in the UV−vis region is not sufficient. Thus, time-resolved spectroscopic methods sensitive to the molecular structure, which is expected to change upon the delocalization of charge, must be employed.

Recently, our research group investigated the oxidized or reduced functional molecules by means of time-resolved resonance Raman (TR^3) measurement during pulse radiolysis.[13−15] Structural changes upon one-electron oxidation and reduction caused by electron beam irradiation have been successfully detected in these studies. In the present study, we applied TR^3 measurements to radical cations and radical anions of St derivatives (Figure 1). Although Raman spectra of the radical cation and radical anion of pristine St have been reported,[16−24] reports on the Raman spectra of oxidized or reduced substituted St are scarce. In the first part of the present paper, we discussed the electronic transitions of oxidized and reduced St derivatives, a large part of which were measured for the first time, and absorption peaks are assigned on the basis of theoretical calculations that included solvent effects. In the second part of the paper, TR^3 spectra of radical ion species of St derivatives were measured during pulse radiolysis. It was found that the substituents exert significant effects on the position of

Received: April 30, 2015
Revised: June 2, 2015
Published: June 8, 2015

DOI: 10.1021/acs.jpca.5b04127
J. Phys. Chem. A 2015, 119, 6816−6822

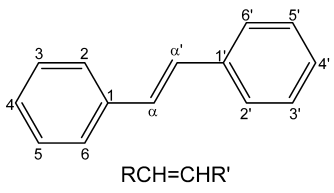

	R	R'
St (1)	C_6H_5	C_6H_5
MSt (2)	4-$CH_3C_6H_4$	C_6H_5
DMSt (3)	4-$CH_3C_6H_4$	4-$CH_3C_6H_4$
MOSt (4)	4-$CH_3OC_6H_4$	C_6H_5
24DMOSt (5)	2,4-$(CH_3O)_2C_6H_3$	C_6H_5
33DMOSt (6)	3-$CH_3OC_6H_4$	3-$CH_3OC_6H_4$
34DMOSt (7)	3,4-$(CH_3O)_2C_6H_3$	C_6H_5
35DMOSt (8)	3,5-$(CH_3O)_2C_6H_3$	C_6H_5
44DMOSt (9)	4-$CH_3OC_6H_4$	4-$CH_3OC_6H_4$

Figure 1. Molecular structures of St derivatives in this study. Numbers in the parentheses are used in Figure 6 to identify the compounds.

the Raman peaks. These substituent effects were discussed on the basis of the electronic nature of the substituents with the help of theoretical calculations. This information will be important for understanding charge delocalization, which is essential in photoinduced charges in conductive materials and photochemical reactivities of radical ion species of aromatic compounds.

EXPERIMENTAL METHODS

Materials. St derivatives in the present study were synthesized according to the procedures indicated in the previous study.[10−12] Solvents were of the best grade commercially available.

Pulse Radiolysis. Transient absorption and TR^3 spectra measurements were performed during pulse radiolysis as described in the previous reports.[13] In TR^3 spectra measurements, a 532 nm nanosecond laser pulse was used as the probe.

Theoretical Calculation. Optimized structures and Raman spectra of the present St derivatives in the neutral and radical ion states were estimated by using density functional theory (DFT) at the (U)B3LYP/6-311+G(d,p) level. The excitation energies of the radical ions were estimated using time-dependent DFT (TDDFT) at the (U)B3LYP/6-311+G(d,p) level. Solvent effects on the absorption spectra of radical ion species were studied by self-consistent reaction field (SCRF) theory using conductor-like polarizable continuum model (CPCM). Calculation results using SCRF(CPCM) are indicated in figure captions and table footnotes. All theoretical calculations were performed using Gaussian 09 package.[25] It was confirmed that the estimated structures did not exhibit imaginary frequency. Theoretically calculated Raman peak positions were corrected by using a factor of 0.97.

RESULTS AND DISCUSSION

Absorption Spectra of Radical Ions of St Derivatives. Radical ions of St derivatives were generated by pulse radiolysis in this study. Figures 2 and, in the Supporting Information, S1 show the transient absorption spectra of St derivatives in 1,2-dichloroethane (DCE) during the pulse radiolysis. At 50 ns after the electron pulse, sufficient formation of radical cations was confirmed in each case. The absorption spectra of the radical cations of St derivatives are similar to that of $St^{\bullet+}$, which showed clear peaks in the visible (483 nm) and near-IR (764 nm) regions. These spectra of St derivatives were in good agreement with previous results,[12] although an explanation of these spectra has not been provided on the basis of molecular orbital (MO) theory. To obtain a better understanding of the electronic transitions of radical ion species, theoretical calculations were performed by using TDDFT at the UB3LYP/6-311+G(d,p) level. The red bars in Figure 2 are the calculated oscillator strengths, which are summarized in

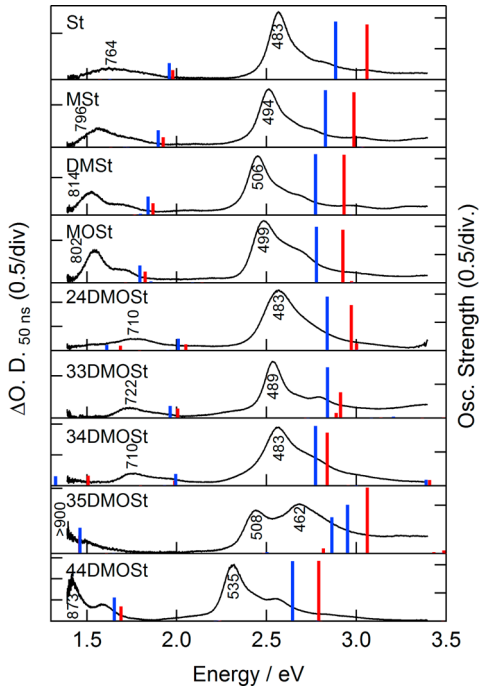

Figure 2. Transient absorption spectra of the radical cations of St derivatives measured at 50 ns after electron pulse during pulse radiolysis of St derivatives (~5 mM) in DCE. Numbers near absorption peaks indicate peak positions in nanometers. Oscillator strengths calculated by TDDFT at the UB3LPY/6-311+G(d,p) level for the radical cations of the St derivatives were indicated by red bars. Oscillator strengths calculated for DCE solvent using SCRF(CPCM) were indicated by blue bars.

Table 1. Energy Levels of HOMO(α) and LUMO(α) and HOMO(α)−LUMO(α) Gap of Radical Cations of St Derivatives in 1,2-Dichloroethane[a]

	HOMO(α)	LUMO(α)	Δ(LUMO(α)−HOMO(α))
St	−7.245 (−)	−3.529 (−)	3.716 (−)
MSt	−7.067 (0.178)	−3.413 (0.116)	3.654 (−0.062)
DMSt	−6.902 (0.343)	−3.310 (0.219)	3.592 (−0.124)
MOSt	−6.808 (0.437)	−3.214 (0.315)	3.594 (−0.122)
24DMOSt	−6.636 (0.609)	−2.976 (0.553)	3.660 (−0.056)
33DMOSt	−7.099 (0.146)	−3.397 (0.132)	3.702 (−0.014)
34DMOSt	−6.706 (0.539)	−3.087 (0.442)	3.619 (−0.097)
35DMOSt	−7.183 (0.062)	−3.418 (0.111)	3.765 (0.049)
44DMOSt	−6.439 (0.806)	−3.005 (0.524)	3.434 (−0.282)

[a]Calculated at UB3LYP/6-311+G(d,p) level using SCRF(CPCM). Unit: electronvolts. Numbers in parentheses are difference from $St^{\bullet+}$.

Table S1 in the Supporting Information. By introducing a solvent effect to the theoretical calculations by using SCRF-

DOI: 10.1021/acs.jpca.5b04127
J. Phys. Chem. A 2015, 119, 6816−6822

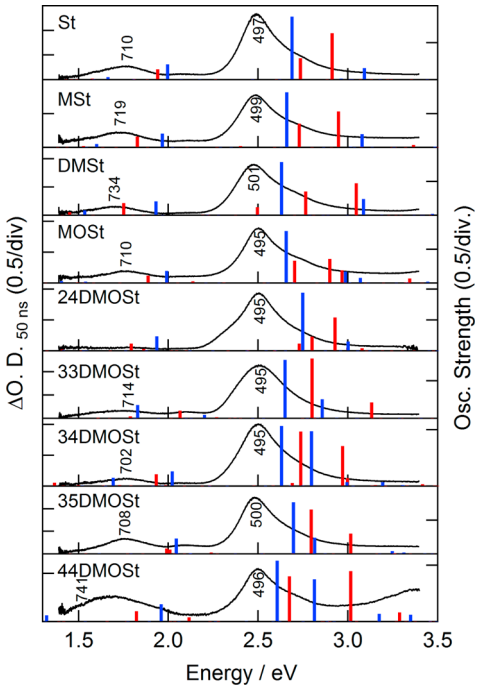

Figure 3. Transient absorption spectra of the radical anions of St derivatives measured at 50 ns after electron pulse during pulse radiolysis of St derivatives (~5 mM) in DMF. Numbers near absorption peaks indicate peak positions in nanometers. Oscillator strengths calculated by TDDFT at the UB3LPY/6-311+G(d,p) level for the radical anions of the St derivatives were indicated by red bars. Oscillator strengths calculated for DMF solvent using SCRF(CPCM) were indicated by blue bars.

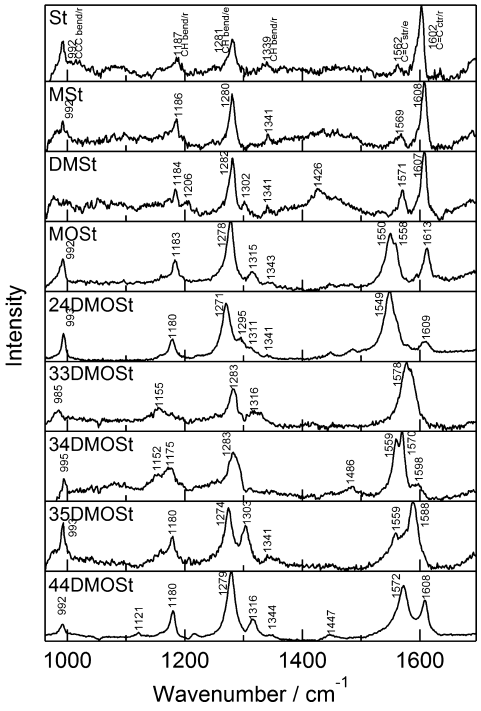

Figure 4. TR^3 spectra of the radical cations of St derivatives measured at 50 ns after pulse during pulse radiolysis of St derivatives in DCE. Numbers indicate the peak positions in inverse centimeters.

(CPCM), the agreement between the calculation and the experiments improved as shown by the blue bars in Figure 2

Table 2. Theoretically Calculated Dihedral Angles (ϕ: $C_{\alpha'}C_{\alpha}C_1C_2$, ϕ': $C_{\alpha}C_{\alpha'}C_{1'}C_{2'}$) of St Derivatives in the Neutral, Radical Cation, and Radical Anion States[a]

	neutral		radical cation		radical anion	
	ϕ	ϕ'	ϕ	ϕ'	ϕ	ϕ'
St	0.00	0.00	0.00	0.00	0.00	0.00
MSt	1.09	1.17	0.00	−0.00	−0.00	−0.00
DMSt	2.48	2.48	0.24	0.24	0.00	0.00
MOSt	4.62	4.72	−0.00	−0.00	−0.00	0.00
24DMOSt	−0.69	−2.97	−0.00	−0.00	0.55	0.02
33DMOSt	−0.03	−0.03	−0.01	−0.01	−0.04	−0.04
34DMOSt	0.00	−0.00	0.00	−0.00	0.00	0.00
35DMOSt	−0.00	0.00	−0.00	0.00	0.00	0.00
44DMOSt	−0.00	−0.00	−0.00	−0.00	−0.00	−0.00

[a]Calculated at UB3LYP/6-311+G(d,p) level. Unit: degree.

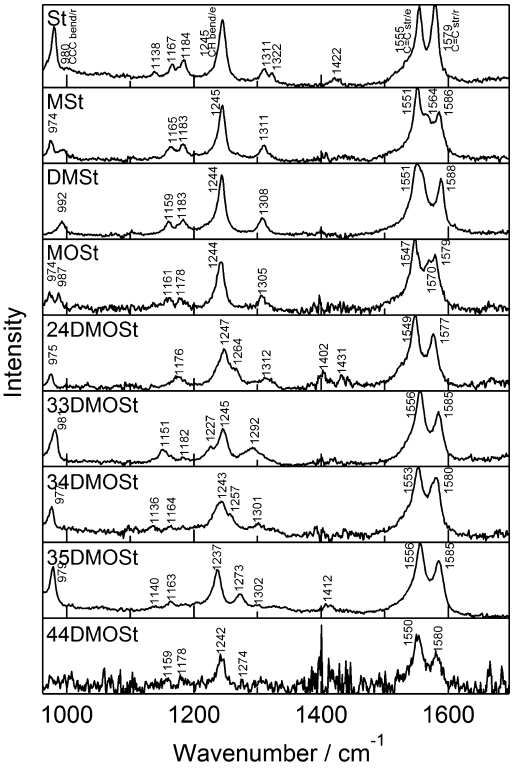

Figure 5. TR^3 spectra of the radical anions of St derivatives measured at 50 ns after pulse during pulse radiolysis of St derivatives in DMF. Numbers indicate the peak positions in inverse centimeters.

and, in the Supporting Information, Table S2. Although theoretical calculations including more sophisticated solvent model will possibly improve the agreements between them furthermore, we did not try this in the present study. In spite of some systematic difference between the calculation and the experimental results, the oscillator strengths calculated using SCRF(CPCM) reasonably explained the absorption spectra of the radical cations. Theoretical calculation on $St^{\bullet+}$ indicated that the electronic transitions, which provided peaks in the near-IR and visible regions, correspond to the third and fourth excited states, respectively, and the oscillator strengths of the lowest and second excited states are negligible. For bis-(methoxy)-substituted St derivatives, the near-IR bands are attributed to the lowest excited state except for $44DMOST^{\bullet+}$, while for other St derivatives the near-IR bands are the second

DOI: 10.1021/acs.jpca.5b04127
J. Phys. Chem. A 2015, 119, 6816−6822

Table 3. Bond Length Change and Shift in the CC Stretching Mode of the Ethylenic Bond of St Derivatives upon Oxidation and Reduction as well as Sum of the Hammett's σ and Bond Length in the Neutral Form Estimated by Density Functional Theory Calculations

	$\sum\sigma^a$	neutral	radical cation		radical anion	
		l/Å^b	$-\Delta\nu$/cm^{-1} ^{c}	Δl/Å^d	$-\Delta\nu$/cm^{-1} ^{c}	Δl/Å^d
St	0.000	1.3455	76	0.0416	83	0.0480
MSt	−0.170	1.3458	68	0.0401	86	0.0471
DMSt	−0.340	1.3460	64	0.0392	84	0.0462
MOSt	−0.268	1.3461	87	0.0366	89	0.0474
24DMOSt		1.3493	83	0.0365	83	0.0451
33DMOSt	0.230	1.3456	59	0.0315	81	0.0497
34DMOSt	−0.153	1.3458	76	0.0299	82	0.0478
35DMOSt	0.230	1.3453	78	0.0354	81	0.0493
44DMOSt	−0.536	1.3464	63	0.0354	85	0.0469

^{a}Sum of Hammett's σ. ^{b}Theoretically calculated bond length of ethylenic group in the neutral form. ^{c}Shift of CC stretching mode of ethylenic bond upon oxidation or reduction. ^{d}Theoretically calculated bond length change of ethylenic group upon oxidation or reduction.

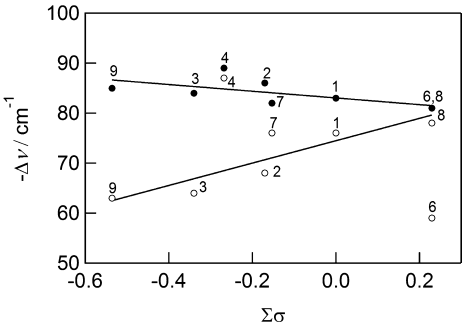

Figure 6. Relation between Raman peaks shift (CC stretching of ethylenic bond) upon (○) oxidation or (●) reduction and sum of Hammett's σ. Numbers close to the circles indicate the compounds number indicated in Figure 1. The fitted lines were estimated by tentatively assuming the linear relation between $\Delta\nu$ and $\sum\sigma$. For radical cation, data points 4 and 6 were excluded from the fitting.

or third excited states in the presence of the solvent (DCE) on the basis of SCRF(CPCM). In addition, the near-IR bands are assigned to the transitions from HOMO-$n(\beta)$ ($n \geq 1$) to HOMO(β) (HOMO = highest occupied molecular orbital), while the visible bands are assigned to the transition from HOMO(α) to LUMO(α) (LUMO = lowest unoccupied molecular orbital). In the case of 35DMOSt$^{\bullet+}$, two peaks appeared in the visible region, which can be assigned to the fifth and sixth excited states, respectively, to which the transitions from HOMO−1(α) to LUMO(α) and HOMO(α) to LUMO-(α) contributed.

As shown in Figure 2, the peak position of the visible bands depends on the substitution patterns. Since the visible band relates to the transition from HOMO(α) to LUMO(α), these energy levels and the HOMO(α)−LUMO(α) gap in DCE are summarized in Table 1. In Table 1, the difference from those of St$^{\bullet+}$ are also indicated in the parentheses. Upon the substitution of methyl or methoxy groups, the energy levels of both HOMO(α) to LUMO(α) increased. Except for 35DMOSt, the increase in the HOMO(α) levels is larger than that of the LUMO(α) levels, which caused a lower energy shift of the visible band, while a higher energy shift was confirmed for 35DMOSt, as indicated in Table 1.

The radical anions of St derivatives were also generated by pulse radiolysis using dimethylformamide (DMF) as the solvent, as shown in Figures 3 and, in the Supporting

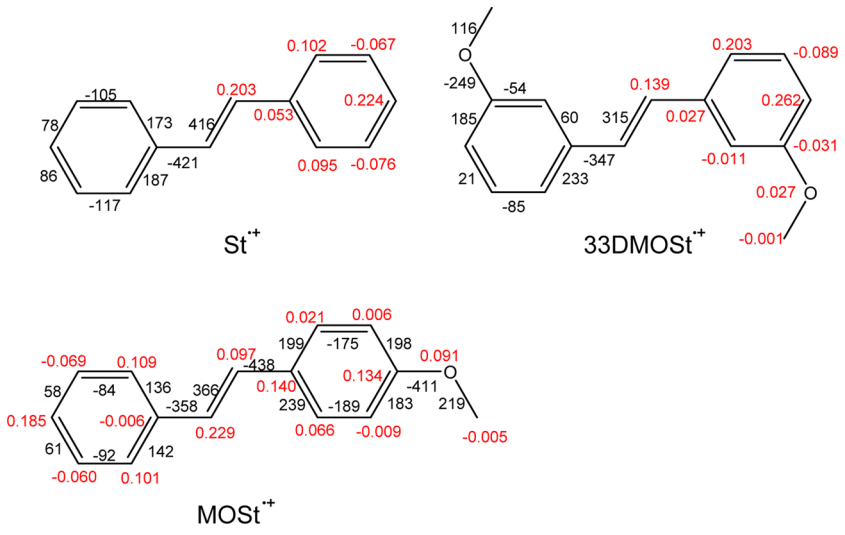

Figure 7. Theoretically calculated spin density of radical cations of St, 33DMOSt, and MOSt. Red numbers close to atom indicate spin densities. Black numbers close to bond are bond length changes upon oxidation in 1×10^{-4} Å unit. From the symmetrical reason a parts of parameters are shown.

DOI: 10.1021/acs.jpca.5b04127
J. Phys. Chem. A 2015, 119, 6816−6822

Information, S2. The spectral shape for $St^{\bullet-}$ is the same as that reported previously,[9] while other radical anions were measured for the first time. Notably, the radical anions of St derivatives exhibit near-IR and visible absorption bands at wavelengths (energies) similar to those of $St^{\bullet-}$; that is, the substituent effects are not large when compared with those of the radical cations. The electronic transitions, which are responsible to the observed absorption bands, are estimated by TDDFT calculations, as summarized in Supporting Information Tables S3 and S4. Here too, by including the solvent effects, rather good agreements between the calculations and the experiments were obtained. It was suggested that the near-IR bands of the radical anions can be attributed mainly to transitions from HOMO(α) to LUMO+n(α) ($n > 1$), and that these are not the lowest excited state (D_1 state). The absorption peaks in the visible region can be attributed mainly to the transition from HOMO−1(β) to HOMO(β), which also includes transitions from HOMO(α) to LUMO+n(α) ($n > 1$). Because the HOMO−1 and HOMO of radical anions are the HOMO and LUMO of the neutral molecules, respectively, it was concluded that the transitions originating from HOMO to LUMO transition of the neutral molecules are responsible for the visible bands of the radical cations and radical anions.

Raman Spectra of Radical Ions of St Derivatives. Because both the radical cations and radical anions of St derivatives exhibited absorbances around 530 nm, the TR^3 spectra were measured using a 532 nm pulse laser as the probe. Figure 4 shows the TR^3 spectra observed at 50 ns after the electron pulse during pulse radiolysis of St derivatives in DCE. In the case of St, the spectrum shown in Figure 4 coincides with the reported spectra of the St radical cation.[20,21] For other St derivatives, the TR^3 spectra of the radical cation species were observed for the first time (Figure 4). For comparison, the Raman spectra of neutral molecules are shown in Figure S3 in the Supporting Information. Assignments of the observed peaks based on the previous report and theoretical calculations are provided in Supporting Information Tables S5 and S6 for the neutral and radical cation forms, respectively.[21] In the case of the St radical cation, the most prominent peaks appeared at 1602, 1281, and 992 cm^{-1}, which are attributed to CC stretching of the ring, CH bending coupled with CC stretching of the ethylenic group, and CCC bending of the ring, respectively. The peaks at 1339 and 1187 cm^{-1} are due to in-plane CH bending of the ring. The absence of the out-of-ring vibrational mode indicates that the radical cation maintains a planar structure in the radical cation state. The small peak at 1562 cm^{-1} is due to the CC stretching of the ethylenic group, which indicates substantial downshift by 76 cm^{-1} when compared to that of the neutral form (Supporting Information, Figure S3 and Table S5), whereas the shift observed with the CC stretching mode (~1600 cm^{-1}) of the ring is not significant (5 cm^{-1} upshift upon oxidation). For other St derivatives, although unsymmetrical substitutions to the phenyl rings increased the number of Raman peaks, similar spectral patterns were confirmed. Although the peak positions of the CH bending modes of the ethylenic and ring groups do not show significant dependence on the substituents, the peaks due to the CC stretching at ~1500−1600 cm^{-1} showed rather large variations. The planar structures of the radical cations of St derivatives are also indicated by the absence of the out-of-plane bending modes. These findings are supported by the theoretical calculations (Table 2): in the radical cation form, the dihedral angles formed by the ethylenic bond and phenyl ring are <0.1° except for DMSt (0.24°), whereas the corresponding angles of the neutral forms are <4.8°.

Raman spectra of the radical anion of St derivatives were obtained by TR^3 measurements during the pulse radiolysis of St derivatives in DMF. Figure 5 shows the spectra at 50 ns after electron pulse irradiation. In the case of the St radical anion, strong peaks are observed at 1579, 1555, 1245, and 980 cm^{-1}. The peak at 1579 cm^{-1} can be attributed to the CC stretching mode of the phenyl ring, while the peak at 1555 cm^{-1} is attributable to the CC stretching of the ethylenic bond. The 1245 cm^{-1} peak is due to the CH bending coupled with CC stretching of the ethylenic bond. The 980 cm^{-1} peak is due to the CCC bend of the phenyl ring. The CC stretching mode of the ethylenic bond showed a significant downshift, as large as 83 cm^{-1} upon reduction. The Raman peaks of radical anions of other St derivatives were assigned on the basis of the previous studies and theoretical calculations, as given in Table S7 in the Supporting Information.[21] The planar structures of the radical anions are indicated by the absence of the out-of-plane bending modes and theoretical calculations (Table 2); the structures show that the dihedral angles formed by the ethylenic bond and phenyl ring are <0.1°, except for 24DMOSt (0.55°) in the radical anion state. It was also confirmed that the substitution of the phenyl ring of the St unit varied the peak positions of the Raman peaks. In particular, the Raman peak around 1550 cm^{-1} due to the CC stretching of the ethylenic bond is sensitive to the substituents.

As indicated in the above sections, the Raman bands due to CC stretching of the ethylenic group showed substantial downshifts upon one-electron oxidation and reduction, indicating that the both oxidation and reduction lowered the bonding order of the ethylenic group. The substituents on the phenyl groups are expected to affect the bonding order of the ethylenic group through their electron-donating or electron-withdrawing properties. A decrease in the bonding order upon oxidation or reduction is apparent in the elongation of the bond length of the ethylenic group (Δl, Table 3). In Figure 6, the shifts of the peak positions of CC stretching of the ethylenic group upon oxidation or reduction ($\Delta\nu$) are plotted against the sum of Hammett's σs ($\sum\sigma$),[26] a parameter that indicates the electron-donating or electron-withdrawing nature of the substituents. In the case of radical cations of St derivatives, $\Delta\nu$ tends to become larger with increasing $\sum\sigma$ values. This trend seems to be reasonable when the electron-withdrawing nature lowers the bonding order of the ethylenic group in the radical cation. On the other hand, in the case of radical anions, $\Delta\nu$ tends to become smaller with increasing $\sum\sigma$ values, although the dependence is not very significant when compared to that of the radical cation. The smaller $\Delta\nu$ with a larger $\sum\sigma$ is also reasonable, because in the radical anion the electron-withdrawing nature of the substituents increases the bonding order of the ethylenic group by reducing the electron density in the antibonding MO.

It is obvious from Figure 6 that the $\Delta\nu$ value of the 33DMOSt radical cation is smaller than expected from the $\sum\sigma$ value, indicating that the bonding order is not lower than expected. To confirm this, the theoretically calculated spin density of the ethylenic group of radical cation 33DMOSt was compared with that of St in Figure 7. Obviously, the spin density of the ethylenic group of 33DMOSt is lower than that of St, supporting the view that the higher bonding order of the 33DMOSt radical cation leads to a smaller $\Delta\nu$ than St radical cation. On the other hand, in the case of the MOSt radical

DOI: 10.1021/acs.jpca.5b04127
J. Phys. Chem. A 2015, 119, 6816−6822

cation, the enhancement of the double bonding nature of the bond connecting the O and C of the phenyl ring (Figure 7) seems to make the bonding order of ethylenic group lower, resulting in a downshift that is larger than expected.

As indicated above, the $\Delta\nu$ of the radical anion is less sensitive to $\sum\sigma$ when compared to that of the radical cation. For St derivatives in the present study, the average spin density of the ethylenic carbon was within 0.148−0.172 for the radical anions, while that of the radical cation was within 0.133−0.203. Thus, the wide variation in the spin densities of the radical cation reflected the wide variation in the bonding order, that is, variation in $\Delta\nu$, of the radical cation.

CONCLUSIONS

The radical cations and radical anions of St derivatives were investigated by radiation chemical methods. Transient absorption measurements during pulse radiolysis provided the absorption spectra of the radical ion states; theoretical calculations gave reasonable peak assignments. The variation in the peak position was explained by the positions of the HOMO and LUMO. Structural changes upon oxidation and reduction were detected with TR^3 measurements during pulse radiolysis. Significant downshifts were observed with the CC stretching mode of the ethylenic groups, indicative of the decrease in the bonding order. Especially, a significant downshift was observed upon reduction. On the other hand, the extent of the downshift caused by oxidation depends largely on the electron-donating or electron-withdrawing nature of the substituents.

ASSOCIATED CONTENT

Supporting Information

Transient absorption spectra, calculated excitation energies, Raman spectra of neutral states, assignments of the Raman peaks, and complete authors list of ref 25. The Supporting Information is available free of charge on the ACS Publications website at DOI: 10.1021/acs.jpca.5b04127.

AUTHOR INFORMATION

Corresponding Authors

*E-mail: fuji@sanken.osaka-u.ac.jp. +81-6-6879-8495. (T.M.)
*E-mail: majima@sanken.osaka-u.ac.jp. Phone: +81-6-6879-8496. (M.F.)

Notes

The authors declare no competing financial interest.

ACKNOWLEDGMENTS

We thank the members of the Research Laboratory for Quantum Beam Science of SANKEN, Osaka University. This work was partly supported by a Grant-in-Aid for Scientific Research (Project Nos. 25220806, 25288035, and others) from the Ministry of Education, Culture, Sports, Science and Technology (MEXT) of Japanese Government.

REFERENCES

(1) Hamaguchi, H. Transient Raman Studies of the Cis-Trans Photoisomerization Processes in Stilbene and Retinal. *J. Mol. Struct.* **1985**, *126*, 125−32.
(2) Meier, H. Photochemistry of Stilbenoid Compounds and Their Role in Materials Technology. *Angew. Chem., Int. Ed. Engl.* **1992**, *31*, 1437−1456.
(3) Whitten, D. G. Photochemistry and Photophysics of Trans-Stilbene and Related Alkenes in Surfactant Assemblies. *Acc. Chem. Res.* **1993**, *26*, 502−9.
(4) Goerner, H.; Kuhn, H. J. Cis-Trans Photoisomerization of Stilbenes and Stilbene-Like Molecules. *Adv. Photochem.* **1995**, *19*, 1−117.
(5) Arai, T. Photochemical Cis-Trans Isomerization in the Triplet State. *Mol. Supramol. Photochem.* **1999**, *3*, 131−167.
(6) Gilbert, A. Cyclization of Stilbene and Its Derivatives. In *CRC Handbook of Organic Photochemistry and Photobiology,* 2nd ed.; CRC Press LLC: Boca Raton, FL, 2004; pp 33/1−33/11.
(7) Mori, T.; Inoue, Y. C═C Photoinduced Isomerization Reactions. *Mol. Supramol. Photochem.* **2005**, *12*, 417−452.
(8) Conjugated Polymers, Theory, Synthesis, Properties, and Characterization. In *Handbook of Conducting Polymers,* 3rd ed.; Skotheim, T. A., Reynolds, J. R., Eds.; CRC Press LLC: Boca Raton, FL, 2007.
(9) Shida, T. *Electronic Absorption Spectra of Radical Ions;* Elsevier: New York, 1988.
(10) Tojo, S.; Morishima, K.; Ishida, A.; Majima, T.; Takamuku, S. Remarkable Enhancements of Isomerization and Oxidation of Radical Cations of Stilbene Derivatives Induced by Charge-Spin Separation. *J. Org. Chem.* **1995**, *60*, 4684−4685.
(11) Majima, T.; Tojo, S.; Ishida, A.; Takamuku, S. Cis−Trans Isomerization and Oxidation of Radical Cations of Stilbene Derivatives. *J. Org. Chem.* **1996**, *61*, 7793−7800.
(12) Majima, T.; Tojo, S.; Ishida, A.; Takamuku, S. Reactivities of Isomerization, Oxidation, and Dimerization of Radical Cations of Stilbene Derivatives. *J. Phys. Chem.* **1996**, *100*, 13615−13623.
(13) Fujitsuka, M.; Cho, D. W.; Tojo, S.; Choi, J.; Huang, H.-H.; Yang, J.-S.; Majima, T. Radical Cation of Star-Shaped Condensed Oligofluorenes Having Isotruxene as a Core: Importance of Rigid Planar Structure on Charge Delocalization. *J. Phys. Chem. A* **2014**, *118*, 2307−2315.
(14) Choi, J.; Cho, D. W.; Tojo, S.; Fujitsuka, M.; Majima, T. Configurational Changes of Heme Followed by Cytochrome c Folding Reaction. *Mol. BioSyst.* **2015**, *11*, 218−222.
(15) Choi, J.; Cho, D. W.; Tojo, S.; Fujitsuka, M.; Majima, T. Structural Study of Various Substituted Biphenyls and Their Radical Anions Based on Time-Resolved Resonance Raman Spectroscopy Combined with Pulse Radiolysis. *J. Phys. Chem. A* **2015**, *119*, 851−856.
(16) Takahashi, C.; Maeda, S. Raman Spectra of Stilbene Negative Ions in Tetrahydrofuran Solution. *Chem. Phys. Lett.* **1974**, *28*, 22−26.
(17) Dosser, L. R.; Pallix, J. B.; Atkinson, G. H.; Wang, H. C.; Levin, G.; Szwarc, M. Time-Resolved Resonance Raman (TR^3) Spectroscopy. Structural Identification of an Intermediate in the Photolysis of Trans-Stilbene Dianions. *Chem. Phys. Lett.* **1979**, *62*, 555−561.
(18) Hub, W.; Schneider, S.; Doerr, F.; Simpson, J. T.; Oxman, J. D.; Lewis, F. D. Time-Resolved Resonance Raman Investigation of Photostimulated Electron Transfer from Amines to Trans-Stilbene. *J. Am. Chem. Soc.* **1982**, *104*, 2044−2045.
(19) Hub, W.; Schneider, S.; Doerr, F.; Oxman, J. D.; Lewis, F. D. Trans-Stilbene-Amine Exciplexes. Behavior of the Exciplex, Solvent-Separated Radical Ion Pair, and Free Radical Ions. *J. Am. Chem. Soc.* **1984**, *106*, 708−715.
(20) Hub, W.; Klueter, U.; Schneider, S.; Doerr, F. Time-Resolved Resonance Raman Spectroscopic Investigation of the Trans-Stilbene Cation Radical Kinetics in Photolytically Induced Electron-Transfer Reactions. *J. Phys. Chem.* **1984**, *88*, 2308−2315.
(21) Schneider, S.; Scharnagl, C.; Bug, R.; Baranovic, G.; Meic, Z. A Force Field Calculation for Trans-Stilbene Ion Radicals. *J. Phys. Chem.* **1992**, *96*, 9748−9759.
(22) Negri, F.; Orlandi, G. Quantum Chemical Simulation of the Resonance Raman Spectra of Stilbene Radical Ions: A Test Case for the Study of Charge Carriers in Doped PPV. *J. Mol. Struct.* **2000**, *521*, 197−209.
(23) Nakabayashi, T.; Kamo, S.; Sakuragi, H.; Nishi, N. Time-Resolved Raman Studies of Photoionization of Aromatic Compounds

DOI: 10.1021/acs.jpca.5b04127
J. Phys. Chem. A 2015, 119, 6816−6822

in Polar Solvents: Picosecond Relaxation Dynamics of Aromatic Cation Radicals. *J. Phys. Chem. A* **2001**, *105*, 8605−8614.
(24) Aquino, F. W.; Schatz, G. C. Time-Dependent Density Functional Methods for Raman Spectra in Open-Shell Systems. *J. Phys. Chem. A* **2014**, *118*, 517−525.
(25) Frisch, M. J.; Trucks, G. W.; Schlegel, H. B.; Scuseria, G. E.; Robb, M. A.; Cheeseman, J. R.; Scalmani, G.; Barone, V.; Mennucci, B.; Petersson, G. A., et al. *Gaussian 09, Revision C.01;* Gaussian, Inc.: Wallingford, CT, 2009.
(26) Hammett, L. P. The Effect of Structure Upon the Reactions of Organic Compounds. Benzene Derivatives. *J. Am. Chem. Soc.* **1937**, *59*, 96−103.

DOI: 10.1021/acs.jpca.5b04127
J. Phys. Chem. A 2015, 119, 6816−6822